HHS Public Access

Author manuscript

Math Biosci. Author manuscript; available in PMC 2016 June 01.

Published in final edited form as:

Math Biosci. 2015 June ; 264: 21–28. doi:10.1016/j.mbs.2015.03.001.

Modeling multiple infection of cells by viruses: challenges and insights

Dustin Phan and **Dominik Wodarz***

Department of Ecology and Evolutionary Biology, 321 Steinhaus Hall, University of California, Irvine, CA 92617

Abstract

The multiple infection of cells with several copies of a given virus has been demonstrated in experimental systems, and has been subject to previous mathematical modeling approaches. Such models, especially those based on ordinary differential equations, can be characterized by difficulties and pitfalls. One such difficulty arises from what we refer to as multiple infection cascades. That is, such models subdivide the infected cell population into sub-populations that are carry *i* viruses, and each sub-population can in principle always be further infected to contain i+1 viruses. In order to study the model with numerical simulations, the infection cascade needs to be cut artificially, and this can influence the results. This is shown here in the context of the simplest setting that involves a single, homogeneous virus population. If the viral replication rate is sufficiently fast, then most infected cells will accumulate in the last member of the infection cascade, leading to incorrect numerical results. This can be observed even with relatively long infection cascades, and in this case computational costs associated with a sufficiently long infection cascade can render this approach impractical. We subsequently examine a more complex scenario where two virus types / strains with different fitness are allowed to compete. Again, we find that the length of the infection cascade can have a crucial influence on the results. Competitive exclusion can be observed for shorter infection cascades, while coexistence can be observed for longer infection cascades. More subtly, the length of the infection cascade can influence the equilibrium level of the populations in numerical simulations. Studying the model in a parameter regime where an increase in the infection cascade length does not influence the results, we examine the effect of multiple infection on the outcome of competition. We find that multiple infection can promote coexistence of virus types if there is a degree of intracellular niche separation. If this is not the case, the only outcome is competitive exclusion, similar to equivalent models that do not take into account multiple infection of cells. We further find that multiple infection has a reduced ability to allow coexistence if virus spread is spatially restricted compared to a well-mixed system. These results provide important insights when analyzing and interpreting multiple infection models.

*corresponding author: dwodarz@uci.edu; Tel:949-824-2531; Fax: 949-824-2181.

Keywords

Multiple infection; Competition; Virus dynamics; Mathematical models

1. Introduction

Investigating the dynamics of virus spread through target cell populations has produced a better understanding of the principles underlying virus dynamics and evolution, and has provided insights into in vivo processes that contribute to the development of disease from a variety of human pathogens, such as human immunodeficiency virus (HIV), hepatitis B and C viruses (HBV and HCV). Mathematical models have played an important role in this respect [1; 2; 3]. A relatively underexplored area in virus dynamics is the multiple infection of cells, i.e. the simultaneous infection of a cell with more than one copy of a virus. This can occur in different infections. For example, adenoviruses are thought to infect cells with several viral copies, and interesting dynamics have been observed that appear related to multiple infection and that warrant further investigation with mathematical models [4]. Some of the better documented data come from human immunodeficiency virus (HIV). A collection of in vitro and ex vivo studies clearly showed that more than one virus can enter the same cell [5; 6; 7; 8]. For in vivo scenarios, patient data have been reported that showed an average of 3–4 proviruses per infected cell in the spleen [9]. Other studies, however, argued that the great majority of infected cells in HIV-infected patients in the blood and tissues are singly infected [10; 11]. This discrepancy might be due to the particular T cell subsets examined in the respective studies, although the reason is not understood. The occurrence of viral recombination in vivo, however, further indicates an important role of multiple infection, since recombination would otherwise not be possible [7; 9; 12].

Virus dynamics in the presence of multiple infection has been examined mathematically in a few studies. Basic dynamics were investigated with ordinary differential equations and integro-differential equations by Dixit and Perelson [13; 14], and subsequently investigated further in references [15; 16], using ordinary differential equations and agent-based models. The effect of recombination, which requires multiple infection, has been modeled, e.g. [17; 18; 19]. Competition was also incorporated into multiple infection models [20; 21]. The ordinary differential equations models that have been reported are similar in structure compared to those in the field of epidemiology, where multiple pathogens are assumed to infect hosts [22; 23; 24; 25; 26; 27; 28].

Those models can be characterized by certain difficulties and pitfalls, especially when investigating simplified formulations in terms of ODEs. ODEs that describe multiple infection generally divide the population of infected cells in subpopulations that are infected with one, two, three etc viruses. We refer to this as the “multiple infection cascade”. In principle, this cascade can be infinite. In practical terms, the number of cells infected with a multiplicity that lies above a certain threshold will be negligible, and thus the infection cascade can be truncated. It is, however, unclear how exactly the truncation of the cascade can affect the results. In the presence of competition, it has been shown that certain truncated and simplified model forms can lead to pathological outcomes, where the

assumption of two identical (and thus competitively neutral) pathogens can lead to a unique equilibrium [27].

In this paper, we examine in more detail ODE modeling approaches to study the multiple infection of cells with viruses. We start by investigating how the truncation of the multiple infection cascade can affect the outcome in different parameter regions in the context of basic dynamics. We then expand the multiple infection models to investigate the competition between two virus strains, taking into account both competition for target cells (as in standard virus competition models) and the competition for intracellular resources.

This analysis will be performed in the most general setting, without considering one specific infection. The aim of this work is to gain a better understanding of how model structure can influence outcome in models that describe the multiple infection of cells by viruses. This can form the basis for future work that applies this type of model to specific infections, which will require careful consideration of assumptions that are specific to the virus in question.

2. Results

2.1. Basic ODE models of multiple infection

Mathematical models of virus dynamics are often based on ordinary differential equations, and this approach has also been used to describe the infection of cells by multiple copies of the same virus (multiple infection). Denoting the population of susceptible cells by *S*, free virus by *V*, and the population of cells infected with *i* viruses by I_i, the model is given as follows.

$$\frac{dS}{dt}=\lambda - dS - \beta SV$$

$$\frac{dI_1}{dt}=\beta SV - a_1 I_1 - \beta I_1 V$$

$$\frac{dI_i}{dt}=\beta I_{i-1}V - a_i I_i - \beta I_i V \quad \ldots. \quad \frac{dI_n}{dt}=\beta I_{n-1}V - a_n I_n \qquad (1)$$

$$\frac{dV}{dt}=\sum_{i=1}^{n} k_i I_i - uV$$

This is an extension of basic virus dynamics models [1; 2; 3], and has been described first by Dixit and Perelson [13], with extensions published subsequently [2; 3]. Susceptible target cells are produced with a rate λ and die with a rate d. Infection of susceptible cells by virus occurs with a rate β, generating cells infected with a single copy of the virus. These cells can be infected by further virus particles with a rate β, generating cells infected with *i* copies of the virus. This process can continue until the end of the infection cascade, I_n, is reached.

Cells in this population cannot be infected any further. Infected cell populations die with a rate a_i and produce virus with a rate k_i. Free virus decays with a rate u. In this formulation, the rate of virus production, *k*, and the rate of infected cell death, *a*, can depend on the multiplicity of infection, *i*, although it does not have to. In the simplest form, these parameters do not depend on the multiplicity of infection, as described by [13]. In this case, virus production is determined predominantly by cellular factors, keeping the overall amount of virus produced constant and independent of the number of viruses in the cell. Alternatively, it is possible that the rate of virus production and the death rate of infected cells can increase to a certain degree in multiply infected cells, a scenario considered in [16]. In models that have been applied to HIV infection, it has also been assumed that the ability of a cell to become infected can be lost over time, as a result of e.g. receptor down-modulation [13]. This will not be considered in the present context.

One aspect we would like to explore here is the dependency of the dynamics on model structure. In particular, the ODE formulation requires an arbitrary end to the infection cascade, I_n. The larger the value of *n*, the more computationally expensive simulations of this system become. The value of *n*, however, can impact the dynamics that are observed in this model, and this will be investigated in the following sections. First, it will be assumed that virus parameters are independent of the infection multiplicity. Subsequently, we will assume that multiply infected cells produce more virus during their life-span than singly infected cells.

2.1.1. Virus parameters are independent of infection multiplicity—This system has been studied analytically before, and the reader is referred to these analyses for details [13; 16]. If the basic reproductive ratio of the virus is greater than one, the virus and cell populations converge to an internal, stable equilibrium, which has been defined [13; 16]. Here, we concentrate on the distribution of cells infected with different multiplicities. The most abundant infected cell population are singly infected cells, I_1, and the abundance of multiply infected cells, I_i, are successively lower (Figure 1). The population size of the infected cell sub-populations decline exponentially with increasing multiplicities of infection (Figure 2a), and the rate of this exponential decline is given by $\ln\left(\frac{\beta\lambda - ad}{\beta\lambda - ad - a^2}\right)$, and hence depends on the parameters that determine the basic reproductive ratio of the virus. The faster the basic reproductive ratio of the virus, the slower the rate of decline. In other words, the singly infected cells become less dominant and the distribution becomes more even for faster viral replication kinetics. In the extreme case where the basic reproductive ratio of the virus is very large, all infected cell sub-populations are almost equally abundant.

If the decline of the successive infected cell sub-populations is relatively slow, the modeling approach discussed here can become difficult. If the length of the multiple infection cascade, *n*, is not sufficiently large, the majority of the infected cells will accumulate in the last member of the cascade, i.e. in I_n (Figure 2b). This is clearly an unrealistic feature that can lead to artificial results (explored further below). For fast viral replication rates, it is possible to observe this behavior even if relatively large values of *n* are chosen, making it unlikely that the dynamics can be numerically studied in a realistic way. Such parameter regimes are characterized by a very high average multiplicity of infection in the cells.

2.1.2. Virus parameters depend on infection multiplicity—Here, it will be assumed that the rate of viral replication increases in multiply infected cells. In this case, this also leads to an increase in the burst size of the infected cells (number of viruses produced during the life-span of the cell), which is given by k_i/a_i in the model [26]. For simplicity, it is assumed that only k_i is an increasing function of i, and that the death rate of infected cells remains independent of infection multiplicity. In particular, we will assume that the rate of virus production is given by $k\sum_{i=1}^{n}\frac{i(1+\varepsilon)}{i+\varepsilon}$. The overall rate of virus production is a saturating function of the infection multiplicity. The parameter ε is the saturation constant. This parameter also appears in the numerator to avoid having to re-scale the parameter k if the value of ε is changed. For ε=0, this expression reverts back to the previous model where the rate of virus production was independent of the infection multiplicity. For $\varepsilon\to\infty$,the rate of virus production increases linearly with the infection multiplicity. This extreme case, however, is most likely not realistic and will not be analyzed here. We note that although a simplified scenario is considered in which only the rate of viral replication increases with the multiplicity of infection, the general results that we describe are not dependent on this simplification. The results hold as long as the burst size of infected cells (given by the rate of virus production divided by the infected cell death rate) increases with infection multiplicity. In reality, a higher viral replication rate can lead to a higher rate of infected cell death. As long as the increase in the death rate of infected cells is less than the increase in the viral replication rate at higher infection multiplicities, the burst size increases and our results hold. If the death rate of the infected cells increases more than the replication rate of the virus in multiply infected cells, the burst size of infected cells does not increase, which represents a different regime.

The properties of this type of model have been examined in a previous study [16], and can involve more complex dynamics. In particular, whether the infection is established or not can depend on the initial conditions, and hence, is not determined entirely by the basic reproductive ratio of the virus anymore. If an infection is established, the virus and cell populations again converge to a stable equilibrium, the properties of which have been described before [16]. As in the previous model, the infected cell sub-populations at equilibrium are a declining function of the infection multiplicity, and the decline is again exponential. The exact rate of decline could not be calculated in this system. In contrast to the previous system (model 1), however, there is a stronger tendency for the decline to be relatively slow, leading to a more even distribution of the infected cell sub-populations. The reason is that on average, the virus replicates faster as a result of the higher virus output from multiply infected cells. Hence, the average multiplicity of infection rises more as the replication kinetics of the virus are increased. Therefore, in this model it is easier to enter a parameter regime where most of the infected cells accumulate in the last element of the infection cascade, I_n, leading to difficulties for numerical simulations of this system (Figure 2 c,d).

2.2 Competition dynamics

Competition between different virus strains that infect the same target cell population has been studied with mathematical models, using approaches that are extensions of basic virus

dynamics models that do not take into account multiple infection [1; 3]. In such scenarios, competitive exclusion is typically observed, where the virus strain with the higher basic reproductive ratio wins the competition. As expected from ecological theory, coexistence is observed in models that assume a degree of niche separation between the competing virus strains, such as the infection of different kinds of target cells [29; 30; 31]. Coinfection has been argued to be a mechanism that can promote coexistence [20; 21; 22; 23; 24; 25; 26; 27], both in models that describe the spread of pathogens among hosts, and in models that describe the spread of viruses through cell populations. At the same time, it has been pointed out that model structure can be problematic in this respect [27]. Certain simplified models that are characterized by coexistence of competing strains have the unrealistic feature that a unique equilibrium is attained under the assumption that the two pathogen strains are competitively neutral, i.e. practically indistinguishable. Such models are not a good basis to explore the competition dynamics.

Here, model (1) of the previous section is extended to include two virus strains that compete for the same target cell population. Again, the model includes multiple infection cascades. In this case, cells can be infected with *i* copies of virus strain 1 and *j* copies of virus strain 2, y_{ij}. The model is thus given by the following ordinary differential equations.

$$\frac{dS}{dt}=\lambda - dS - \beta_1 S V_1 - \beta_2 S V_2$$

$$\frac{dI_{10}}{dt}=\beta_1 S V_1 - a_{10} I_{10} - I_{10}(\beta_1 V_1+\beta_2 V_2)$$

$$\frac{dI_{01}}{dt}=\beta_2 S V_2 - a_{01} I_{01} - I_{01}(\beta_1 V_1+\beta_2 V_2)$$

$$\frac{dI_{i,j}}{dt}=\beta_1 I_{i-1,j} V_1+\beta_2 I_{i,j-1} V_2 - a_{i,j} I_{i,j} - I_{i,j}(\beta_1 V_1+\beta_2 V_2) \quad (2)$$

$$\frac{dI_{i+j=n}}{dt}=\beta_1 I_{i-1,j} V_1+\beta_2 I_{i,j-1} V_2 - a_{i,j} I_{i,j}$$

$$\frac{dV_1}{dt}=k_1 \sum_{i=1}^{n}\sum_{j=1}^{n} \frac{(1+\varepsilon)i}{i+c_1 j+\varepsilon} I_{i,j} - u V_1$$

$$\frac{dV_2}{dt}=k_2 \sum_{i=1}^{n}\sum_{j=1}^{n} \frac{(1+\varepsilon)j}{c_2 i+j+\varepsilon} I_{i,j} - u V_2$$

The general model structure is the same as that explained in model (1), except that we now track cells infected with two strains. The rate of virus production in infected cells merits further explanation. In a given cell, progeny virus of stain 1 is produced with a rate $\frac{k(1+\varepsilon)i}{i+c_1 j+\varepsilon}$. This captures competition between the virus strains within a cell. Different viruses or virus strains are likely to use common resources within the cell, thus introducing competition for cellular products. Hence, the rate of virus production of strain 1 is negatively impacted by both the presence of further viruses of the same strain (intraspecific competition, i), and by viruses of the second strain (interspecific competition, j). The relative strength of interspecific competition is captured in the parameter c_1. If $c_1=1$, the negative impact of strain two on strain one is identical to the negative impact of additional strain 1 genomes on themselves. If $c_1<1$, the degree of interspecific competition is reduced. That is, a strain 2 viruses have less of an impact on strain 1 than strain 1 has upon itself. In the extreme case where $c_1=0$, the two virus strains replicate independently within the cell and there is no competition for intracellular resources. If $c_1>1$, a strain 2 virus has a stronger impact on strain 1 than strain 1 viruses have upon themselves. This can be interpreted as direct inhibitory effects. In the extreme case for large values of c_1, strain 1 practically does not produce offspring in cells that are coinfected with both strains. This is a “winner takes it all” situation, where strain 2 is the winner. The same arguments hold for the production rate of virus strain 2, where the parameter c_2 describes the degree of inhibition of strain 2 by the presence of strain 1.

We need to add some more clarifying remarks about the case where $c_{1,2}<1$. If $c_{1,2}=1$, the interpretation is that these are two strains of the same virus. In the opposite extreme, $c_{1,2}=0$ means that they are two separate viruses that infect the same cells. Complete lack of resource sharing means that they replicate by completely separate mechanisms. For $0<c_{1,2}<1$, the situation is intermediate. When we analyzed models for a single virus population, we distinguished between two scenarios: (i) Viral parameters are independent of the infection multiplicity. In this case, the burst size of the infected cell did not depend on the infection multiplicity either. (ii) Viral parameters, and thus the burst size of the infected cells, do depend on infection multiplicity. In the context of two competing viruses, scenario (i) is a little more complex. This is best illustrated for $c_{1,2}=0$. Even if viral parameters are independent of how many copies of this virus reside in the cell, the total burst size of a cell that contains both virus of type 1 and virus of type 2 is higher compared to the burst size of a cell that contains only one virus type. Hence, in this case there is no clear correlation between whether viral parameters do or do not depend on infection multiplicity and the total burst size of infected cells. Similar considerations apply if $0<c_{1,2}<1$. This should be kept in mind in the following sections.

To summarize, this model contains two layers of competition: competition for the common pool of target cells (as assumed in standard virus dynamics models without coinfection), and intracellular competition for resources that are required for viral replication. The balance of these two forces determines the outcome of the competition, which is investigated below. Two virus strains with the following characteristics will be considered. Strain 1 will be the “superior” strain, characterized by a faster replication rate than the “inferior” strain 2 (i.e.

$k_1 > k_2$). This makes strain 1 the better competitor for the target cell pool. This is analogous to a competitive advantage in simpler models that do not allow for multiple infection, and thus allows us to compare how multiple infection modulates the outcome of this competition. For simplicity, all other parameters are assumed to be identical for the two virus strains. In our analysis, we will first assume that multiple infection does not influence viral parameters. Subsequently, this will be examined assuming that the rate of virus replication increases with the multiplicity of infection.

2.2.1. Virus parameters are independent of infection multiplicity—We only consider parameter regions in which each virus strain can persist in isolation. We find that both competitive exclusion and coexistence are possible, depending on the model parameters (Figure 3). Coexistence only occurs if $c<1$. That is, on an intracellular level, a degree of niche separation is required. In other words, the two virus types / virus strains need to utilize the intra-cellular resources in a somewhat different manner. Further, the replication kinetics of the viruses plays an important role. Figure 4 shows the outcome of competition as the virus spread parameters, as well as the parameter c are varied. The rate of virus spread is determined by a variety of parameters. In Figure 4a, we vary the death rate of infected cells, a, and in Figure 4b, we vary infection rate of the viruses, β. A higher infection rate and a lower death rate of infected cells increase the rate of virus spread. We observe that extinction of the inferior competitor is promoted by slower virus spread and by high values of c. For slower virus spread, the equilibrium number of uninfected cells is relatively high, and the equilibrium number of infected cells is relatively low. Therefore, new infections likely result in singly infected cells and multiple infection is not a very important force driving the dynamics. Hence, competition for target cells is the most important determinant of the dynamics, and the properties of the model are similar to those of a model that does not take into account multiple infection. Consequently, competitive exclusion occurs. For faster virus spread, on the other hand, many coinfected cells are generated and the competition for target cells is reduced. Now, intracellular competition becomes an important driving force of the dynamics, and coexistence occurs as long as there is sufficient resource separation between the two virus strains within the cells (value of c below a threshold). How large the coexistence parameter regime is depends on the fitness cost of the inferior virus. In Figure 4a,b, a 5% fitness cost was assumed and coexistence was observed for values of c up to 0.9 (where $c=1$ means complete resource overlap). For higher fitness costs, the coexistence regime is reduced and lower values of c are necessary (Figure 4c, illustrated for the case where the parameter a was varied, c.f. Figure 4a).

So far, we have not examined the assumption of $c_{1,2}>1$, i.e. when there is active interference among the viruses, with the extreme assumption being that the winner takes it all. In this case, the outcome of competition can depend on the initial conditions. A higher initial abundance of one virus strain relative to the other promotes the persistence of this virus strain and the exclusion of the competitor. Thus, if the relative initial abundance of the inferior strain is sufficiently large, it can win the competition. The higher the fitness disadvantage of the inferior strain, the higher its relative initial abundance needs to be for it to win. These patterns have been explored with computer simulations, although they are not

graphically shown here. This dependence on initial conditions is similar that seen in standard Lotka-Volterra competition equations [32].

2.2.2. Virus parameters depend on infection multiplicity—The above analysis was repeated assuming increased viral replication rates in multiply infected cells. The corresponding results are shown in Figure 4d for parameter values that correspond to those used in the last section (compare to Figure 4a). We observe that results are qualitatively similar, but that an increased virus replication rate in multiply infected cells leads to a smaller parameter regime in which coexistence is observed. Faster viral replication in multiply infected cells essentially increases the fitness discrepancy between the two viruses. The superior virus will multiply infect more cells than the inferior virus. Hence it will enjoy the resulting faster replication kinetics in a larger number of cells than the inferior virus. This in turn leads to a more pronounced fitness advantage, explaining the numerical observations.

2.2.3. Effect of the infection cascade length—Section 2.1. examined basic multiple infection dynamics assuming a single virus population. We found that the length of the multiple infection cascade, n, can have an influence on the dynamics especially if the basic reproductive ratio of the virus is relatively large and the average multiplicity of infection is relatively large. In this case it is possible that most infected cells accumulate at the end of the infection cascade, i.e. in I_n. For the competition model, it was assumed that the end of the cascade was reached when $i+j=n$. Because cells at the end of the cascade cannot be infected anymore, the opportunity for multiple infection to occur is reduced, and this can affect the outcome of competition. This is demonstrated in Figure 5. With a relatively large cascade length of n=100, coexistence is observed. With the shortest cascade length (n=2), competitive exclusion occurs. With a cascade length of n=5, the outcome is again coexistence, but the equilibrium levels of the virus populations are different compared to n=100. This shows that the assumed cascade length can have a profound influence not only on the observed dynamics, but also on the qualitative outcome of the interactions between the viruses. Therefore, special attention has to be given to the cascade length when studying such dynamics, ensuring that an increase in n does not lead to different dynamics. This was done in the previous section which analyzed the competition outcomes.

2.3. Effect of space

The previous analysis assumed perfect mixing of populations, i.e. mass action. Here, we consider a spatially explicit model in order to examine the effect of spatial restriction on the outcome of competition. This is done with a stochastic, agent-based model that tracks the fate of individual cells. This modeling approach also eliminates the problem of infection cascades explored in the previous section, because it tracks individual cells and their multiplicity of infection. The model assumes a two-dimensional grid of size $N \times N$, and is described as follows. Each spot in the grid can be empty, contain an uninfected cell, or contain an infected cell that is characterized by its multiplicity of infection. At each time step, N^2 spots of the grid are randomly sampled. If the sampled spot is empty, an uninfected cell can be produced with a probability L. If the sampled spot contains an uninfected cell, it can die with a probability D. If the sampled spot contains an infected cell, the following

actions can occur. The cell can die with a probability A. Alternatively, the cell can attempt to pass on the infection to another cell with a probability B. In this case, a cell within a given neighborhood is randomly chosen as a target for infection. If the chosen spot is empty, no infection occurs. If the chosen spot contains an uninfected cell, it becomes infected with one virus. If the chosen spot contains an already infected cell with a given multiplicity, another virus is added to this cell. The radius around the source cell from which a target cell is chosen can be varied. At one extreme, the target cell can be chosen from all cells in the system, and this corresponds to mass action, also described by the above ODEs. At the other extreme, the target cell is chosen from the eight nearest neighboring cells, and this corresponds to the most stringent degree of spatial restriction. We will compare the dynamics assuming nearest neighbor interactions and mass action.

As before, two virus strains are assumed to be present. Hence, a cell can be infected with i copies of virus 1 and j copies of virus 2. The rate of virus production is determined as follows for each strain present in the cell. For each copy of the virus a target spot is randomly chosen. If the chosen spot contains a susceptible cell, this copy gets passed on with probability $\frac{1+\varepsilon}{i+c_1 j+\varepsilon}$ for strain 1, and $\frac{1+\varepsilon}{c_2 i+j+\varepsilon}$ for strain 2. This corresponds to the same assumptions that were made for the ODEs in the previous sections, and captures the intracellular competition between the virus strains in the same way. As before, if ε=0, virus parameters do not depend on the multiplicity of this virus in the cell. If ε>0, the rate of virus replication increases if multiple copies of this virus infect the cell. For simplicity, we will concentrate our analysis on the ε=0 scenario for the spatial analysis.

In general, for the nearest neighbor scenario, the same types of outcomes are observed as in the mass-action scenario, and the determinants of the outcome are qualitatively identical. This was obtained by extensive numerical simulations of the model (Figure 6a). We were interested in whether the parameter regime under which extinction occurs was smaller or larger for the nearest neighbor situation compared to mass action. Hence, we compared the two scenarios in the following way. We determined the outcome as a function of the infection rate of the virus, B, and the competition parameter *c* (Figure 6a). We then superimposed the extinction parameter regions for the spatial and the non-spatial scenarios in order to compare which one is larger. For this, we note that the spatial model has a higher threshold value of B required to sustain the infection than the mass action model. Thus, to properly compare the extinction regimes for the two scenarios, we subtracted the difference in the threshold values from the B-parameter in the spatial simulations.

The results are shown in Figure 6a. We observe that the extinction regime is larger in the spatial compared to the mass action scenario. In other words, competitive exclusion is promoted by nearest neighbor interactions. The reason for this result is shown in Figure 6b. For the nearest neighbor model, the two virus strains are less likely to meet in the same infected cell. Although multiple infection readily occurs, cells are typically infected with multiple copies of the same virus. Thus, Figure 6b shows that the fraction of cells infected with both virus strains remains significantly lower in the spatial setting compared to the mass action setting. Because the reason for the coexistence is the occurrence of coinfection

with both strains, the coexistence regime is reduced, and extinction occurs over a wider parameter regime.

3. Discussion and Conclusion

This paper examined the use of ordinary differential equations for studying virus dynamics under the assumption that multiple viruses can infect the same cell. We started with basic dynamics where only one, homogeneous virus population exists. Such models have been studied before [13; 16], but we provided a more detailed account of how the length of the infection cascade can influence the results. In general, the number of cells declines exponentially with the multiplicity of infection. How fast the numbers decline, however, depends on the replication rate of the virus. Especially for larger viral replication rates, or for scenarios where the rate of viral replication increases in multiply infected cells, the number of cells harboring i viruses declines relatively slowly with the multiplicity of infection. In this case, most of the cells will accumulate in the last member of the infection cascade even for relatively long cascades, and this can influence the properties of numerical simulations. For such cases, the use of ODEs might be impractical, because very long infection cascades become computationally expensive.

These models were then expanded to study competition dynamics. Previous work has shown that inappropriate model simplification can give rise to pathological results, such as the presence of a unique coexistence equilibrium if two strains are competitively neutral [27]. Here, we show that even if the model is formulated in a way such that this effect is not observed, the outcome of competition can be influenced by the length of the infection cascade. For example, for identical model parameters, competitive exclusion can be observed for shorter infection cascades, while coexistence is observed for longer cascades. There can also be more subtle effects, where the equilibrium population levels that are observed in numerical simulations can vary, depending on the length of the infection cascade. Therefore, when studying such competition dynamics with ODEs, it is important to make sure that a parameter regime is explored in which an increase in the length of the infection cascade does not change the results of numerical simulations.

In this regime, we investigated whether multiple infection can promote the coexistence of two virus stains with different fitness. In equivalent models that do not take into account multiple infection, competitive exclusion tends to be the only outcome [1]. With multiple infection, however, we found that coexistence can occur in the models studied here, but we need to distinguish two levels of competition: competition for target cells, as in previous virus dynamics models that do not take into account multiple infection; and competition for intracellular factors. If the two viruses / virus strains in question use the exact same intracellular resources, i.e. if their intracellular niches completely overlap, then multiple infection cannot lead to the coexistence of the strains. The faster growing strain will win and exclude the slower growing strain. If, on the other hand, there is a degree of niche separation within cells, then multiple infection can allow the coexistence of the different viruses, consistent with general ecological theory [32]. The crucial factor is not the multiple infection in general, but the simultaneous infection of cells by the two different viruses. If a sufficient number of cells harboring both viruses is generated, then coexistence becomes

possible. This in turn can be influenced by assumptions about virus spread. We showed that spatially restricted virus spread leads to lower numbers of cells carrying both viruses because spatial restriction promotes multiple infection of cells with the same virus type rather than the coinfection with both types. Hence, multiple infection promotes coexistence of strains to a lesser degree in a spatial setting compared to a well-mixed system. In general, this analysis indicates that related strains of the same virus are unlikely to coexist in the context of multiple infection, but that multiple infection can promote coexistence of different viruses with separate replication mechanisms that infect the same cells.

Our analysis provides important new insights into the properties of models that describe the multiple infection of cells by viruses. This can form the basis for building such modeling approaches for specific infections, where particular biological realities need to be taken into account for accurate descriptions. An interesting case study to explore would be adenoviruses, where multiple infection is thought to readily occur and where multiple infection is thought to allow the virus to replicate at a faster rate. In a set of experiments a culture of 293 cells, arranged in a 2-dimensional monolayer with agar layover, was infected with an engineered fluorescent adenovirus at very low multiplicities of infection [4]. This allowed the very early spread of the infection from a single infected cell to be monitored over time. It was found that once at least three infected cells were generated, virus spread became significantly faster and the virus population never went extinct anymore. This was inconsistent with the expected extinction probabilities calculated from parameters that were estimated from singly infected cells. Because in the 2D monolayer culture, spread of the virus to nearest neighbors was ensured by agar layover, multiply infected cells became readily generated as soon as the virus had spread to only a few cells. This in turns accelerated the rate of viral replication, accounting for the experimental observations. A better understanding of those growth dynamics, and an investigation of competition dynamics between different virus strains in such a setting, would be important to gain further insights into the spread of adenoviruses, which would also be relevant for human health. This will require multiple infection models that are based on the ones discussed here and that also take into account spatial aspects. Our work provides guidelines for such an analysis. As summarized at the beginning of this article, multiple infection has also been observed with HIV, and a variety interesting questions remain to be explored in this respect. The relevance of multiple infection in vivo, however, has been debated, and there is the additional complication that multiple infection is promoted by direct cell-to-cell transmission through virological synapses [8], which requires different modeling approaches [33].

Acknowledgements

This study was funded in part by NIH grant 1R01AI093998-01

References

1. Nowak, MA.; May, RM. Mathematical principles of immunology and virology. Oxford University Press; 2000. Virus dynamics.
2. Perelson AS. Modelling viral and immune system dynamics. Nature Rev Immunol. 2002; 2:28–36. [PubMed: 11905835]

3. Perelson AS, Ribeiro RM. Modeling the within-host dynamics of HIV infection. BMC Biol. 2013; 11:96. [PubMed: 24020860]
4. Hofacre A, Wodarz D, Komarova NL, Fan H. Early infection and spread of a conditionally replicating adenovirus under conditions of plaque formation. Virology. 2012; 423:89–96. [PubMed: 22192628]
5. Chen J, Dang Q, Unutmaz D, Pathak VK, Maldarelli F, Powell D, Hu WS. Mechanisms of nonrandom human immunodeficiency virus type 1 infection and double infection: preference in virus entry is important but is not the sole factor. J Virol. 2005; 79:4140–4149. [PubMed: 15767415]
6. Dang Q, Chen J, Unutmaz D, Coffin JM, Pathak VK, Powell D, KewalRamani VN, Maldarelli F, Hu WS. Nonrandom HIV-1 infection and double infection via direct and cell-mediated pathways. Proc Natl Acad Sci U S A. 2004; 101:632–637. [PubMed: 14707263]
7. Levy DN, Aldrovandi GM, Kutsch O, Shaw GM. Dynamics of HIV-1 recombination in its natural target cells. Proc Natl Acad Sci U S A. 2004; 101:4204–4209. [PubMed: 15010526]
8. Hubner W, McNerney GP, Chen P, Dale BM, Gordon RE, Chuang FY, Li XD, Asmuth DM, Huser T, Chen BK. Quantitative 3D video microscopy of HIV transfer across T cell virological synapses. Science. 2009; 323:1743–1747. [PubMed: 19325119]
9. Jung A, Maier R, Vartanian JP, Bocharov G, Jung V, Fischer U, Meese E, Wain-Hobson S, Meyerhans A. Multiply infected spleen cells in HIV patients. Nature. 2002; 418:144. [PubMed: 12110879]
10. Josefsson L, King MS, Makitalo B, Brannstrom J, Shao W, Maldarelli F, Kearney MF, Hu WS, Chen J, Gaines H, Mellors JW, Albert J, Coffin JM, Palmer SE. Majority of CD4+ T cells from peripheral blood of HIV-1-infected individuals contain only one HIV DNA molecule. Proc Natl Acad Sci U S A. 2011; 108:11199–11204. [PubMed: 21690402]
11. Josefsson L, Palmer S, Faria NR, Lemey P, Casazza J, Ambrozak D, Kearney M, Shao W, Kottilil S, Sneller M, Mellors J, Coffin JM, Maldarelli F. Single cell analysis of lymph node tissue from HIV-1 infected patients reveals that the majority of CD4+ T-cells contain one HIV-1 DNA molecule. PLoS Pathog. 2013; 9:e1003432. [PubMed: 23818847]
12. Neher RA, Leitner T. Recombination rate and selection strength in HIV intra-patient evolution. PLoS Comput Biol. 2010; 6:e1000660. [PubMed: 20126527]
13. Dixit NM, Perelson AS. HIV dynamics with multiple infections of target cells. Proc Natl Acad Sci U S A. 2005; 102:8198–8203. [PubMed: 15928092]
14. Dixit NM, Perelson AS. Multiplicity of human immunodeficiency virus infections in lymphoid tissue. J Virol. 2004; 78:8942–8945. [PubMed: 15280505]
15. Wodarz D, Levy DN. Effect of different modes of viral spread on the dynamics of multiply infected cells in human immunodeficiency virus infection. J R Soc Interface. 2011; 8:289–300. [PubMed: 20659927]
16. Cummings KW, Levy DN, Wodarz D. Increased burst size in multiply infected cells can alter basic virus dynamics. Biol Direct. 2012; 7:16. [PubMed: 22569346]
17. Bretscher MT, Althaus CL, Muller V, Bonhoeffer S. Recombination in HIV and the evolution of drug resistance: for better or for worse? Bioessays. 2004; 26:180–188. [PubMed: 14745836]
18. Fraser C. HIV recombination: what is the impact on antiretroviral therapy? J R Soc Interface. 2005; 2:489–503. [PubMed: 16849208]
19. Kouyos RD, Otto SP, Bonhoeffer S. Effect of varying epistasis on the evolution of recombination. Genetics. 2006; 173:589–597. [PubMed: 16547114]
20. Wodarz D, Levy DN. Human immunodeficiency virus evolution towards reduced replicative fitness in vivo and the development of AIDS. Proc Biol Sci. 2007; 274:2481–2490. [PubMed: 17666377]
21. Wodarz D, Levy DN. Multiple HIV-1 infection of cells and the evolutionary dynamics of cytotoxic T lymphocyte escape mutants. Evolution. 2009; 63:2326–2339. [PubMed: 19486149]
22. Dietz K. Epidemiologic Interference of Virus Populations. Journal of Mathematical Biology. 1979; 8:291–300. [PubMed: 501225]

23. Gupta S, Swinton J, Anderson RM. Theoretical-Studies of the Effects of Heterogeneity in the Parasite Population on the Transmission Dynamics of Malaria. Proceedings of the Royal Society of London Series B-Biological Sciences. 1994; 256:231–238.
24. Lipsitch M. Vaccination against colonizing bacteria with multiple serotypes. Proceedings of the National Academy of Sciences of the United States of America. 1997; 94:6571–6576. [PubMed: 9177259]
25. Mosquera J, Adler FR. Evolution of virulence: a unified framework for coinfection and superinfection. Journal of Theoretical Biology. 1998; 195:293–313. [PubMed: 9826485]
26. Nowak MA, May RM. Superinfection and the evolution of parasite virulence. Proc R Soc Lond B Biol Sci. 1994; 255:81–89.
27. Lipsitch M, Colijn C, Cohen T, Hanage WP, Fraser C. No coexistence for free: neutral null models for multistrain pathogens. Epidemics. 2009; 1:2–13. [PubMed: 21352747]
28. vanBaalen M, Sabelis MW. The dynamics of multiple infection and the evolution of virulence. American Naturalist. 1995; 146:881–910.
29. Wodarz D. Ecological and evolutionary principles in immunology. Ecol Lett. 2006; 9:694–705. [PubMed: 16706914]
30. Ball CL, Gilchrist MA, Coombs D. Modeling within-host evolution of HIV: mutation, competition and strain replacement. Bull Math Biol. 2007; 69:2361–2385. [PubMed: 17554585]
31. Coombs D, Gilchrist MA, Ball CL. Evaluating the importance of within- and between-host selection pressures on the evolution of chronic pathogens. Theor Popul Biol. 2007; 72:576–591. [PubMed: 17900643]
32. Begon M, Townsend CR, Harper JL. Ecology: from individuals to ecosystems. 2006
33. Komarova NL, Levy DN, Wodarz D. Effect of synaptic transmission on viral fitness in HIV infection. PLoS One. 2012; 7:e48361. [PubMed: 23166585]

Highlights

- Models capturing multiple infection of cells are studied
- Basic dynamics are investigated
- Competition dynamics are investigated
- Details of the model formulation are found to influence results

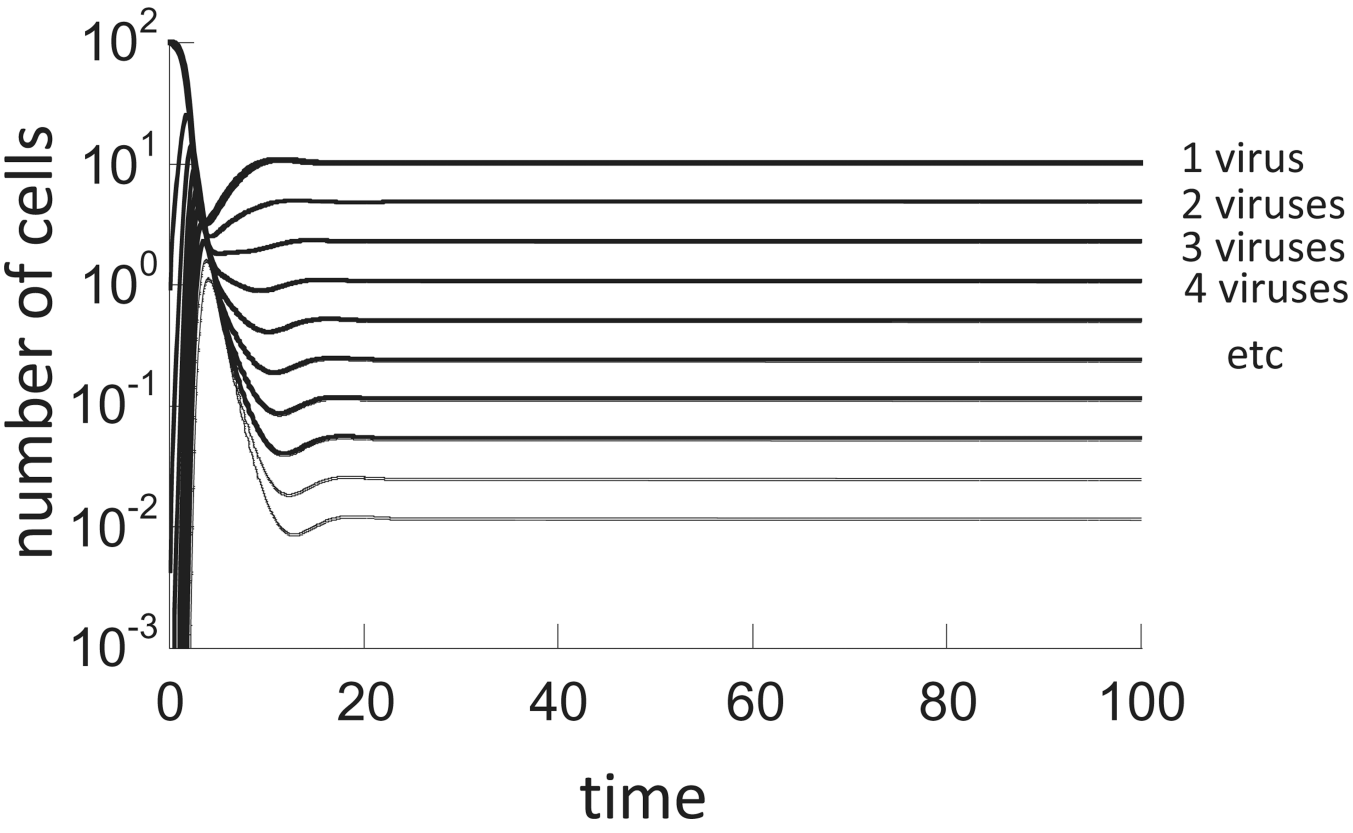

Figure 1.

Distribution of the number of cells infected with *i* viruses, according to model (1) where the rate of virus production does not depend on infection multiplicity. Singly infected cells are most abundant, and the number of cells containing higher infection multiplicities are successively lower. Parameters were chosen as follows. $\lambda=10$; $d=0.1$; $a=1$; $\beta=0.1$; $k=1$; $u=1$; $\varepsilon=0$. Infection cascade length $n=100$.

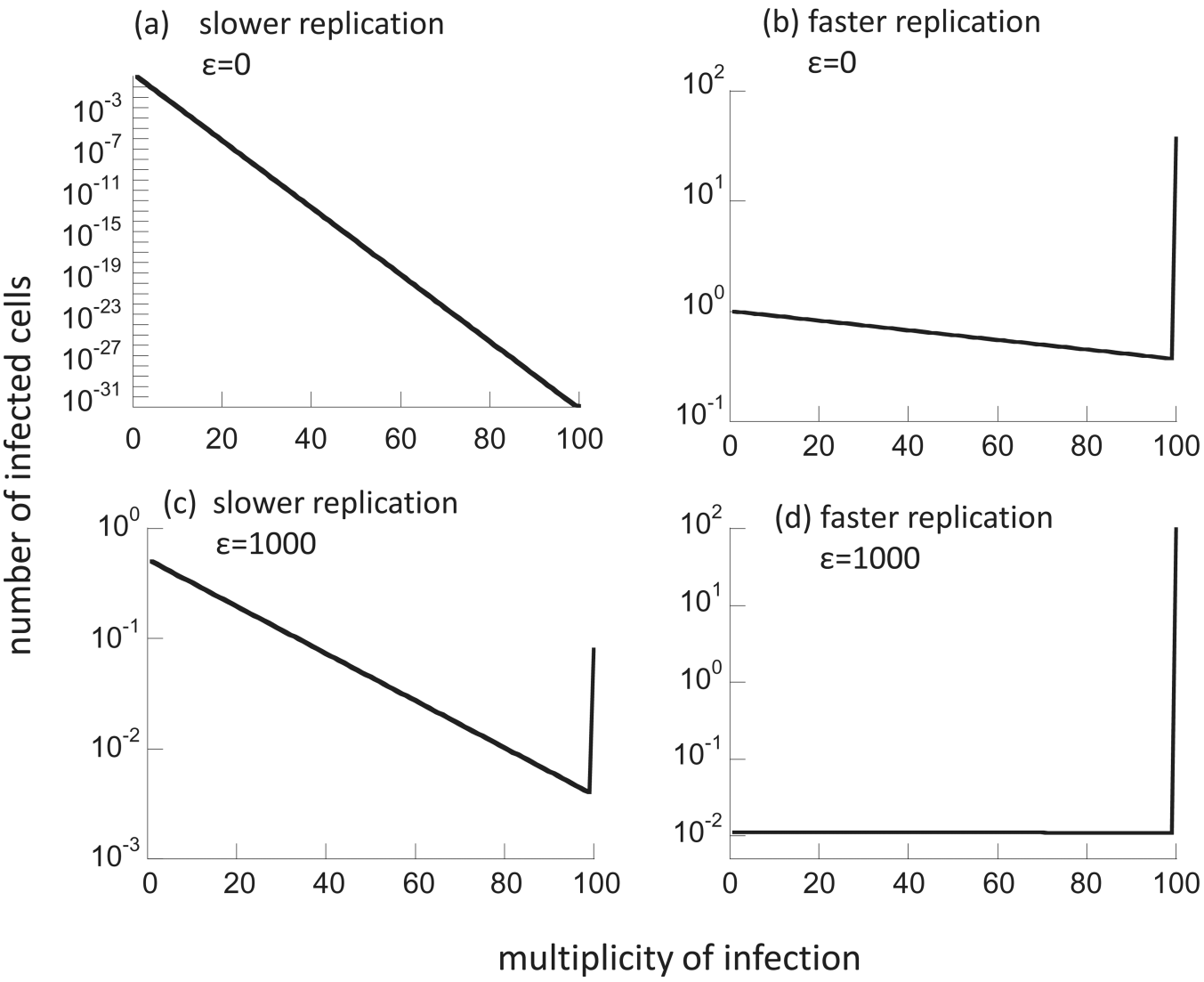

Figure 2.

Equilibrium number of cells as a function of the infection multiplicity, according to model (1). The number of cells declines exponentially with the infection multiplicity. (a) If the rate of viral replication is relatively slow and does not increase with infection multiplicity, the numerical simulations reflect the expected exponential decline. (b) For faster viral replication rates, however, the equilibrium number of cells with increasing infection multiplicity declines much slower, and in numerical simulations, most infected cells accumulate at the end of the infection cascade, giving rise to artificial properties. (c, d) This effect is more pronounced if the rate of viral replication increases for higher infection multiplicities, $\varepsilon>0$. Base parameters were chosen as follows. $\lambda=10$; $d=0.1$; $\beta=0.1$; $k=1$; $u=1$. For (a) $\varepsilon=0$; $a=2$. For (b) $\varepsilon=0$; $a=0.1$. For (c) $\varepsilon=1000$; $a=2$. For (d) $\varepsilon=1000$; $a=0.1$. Infection cascade length $n=100$.

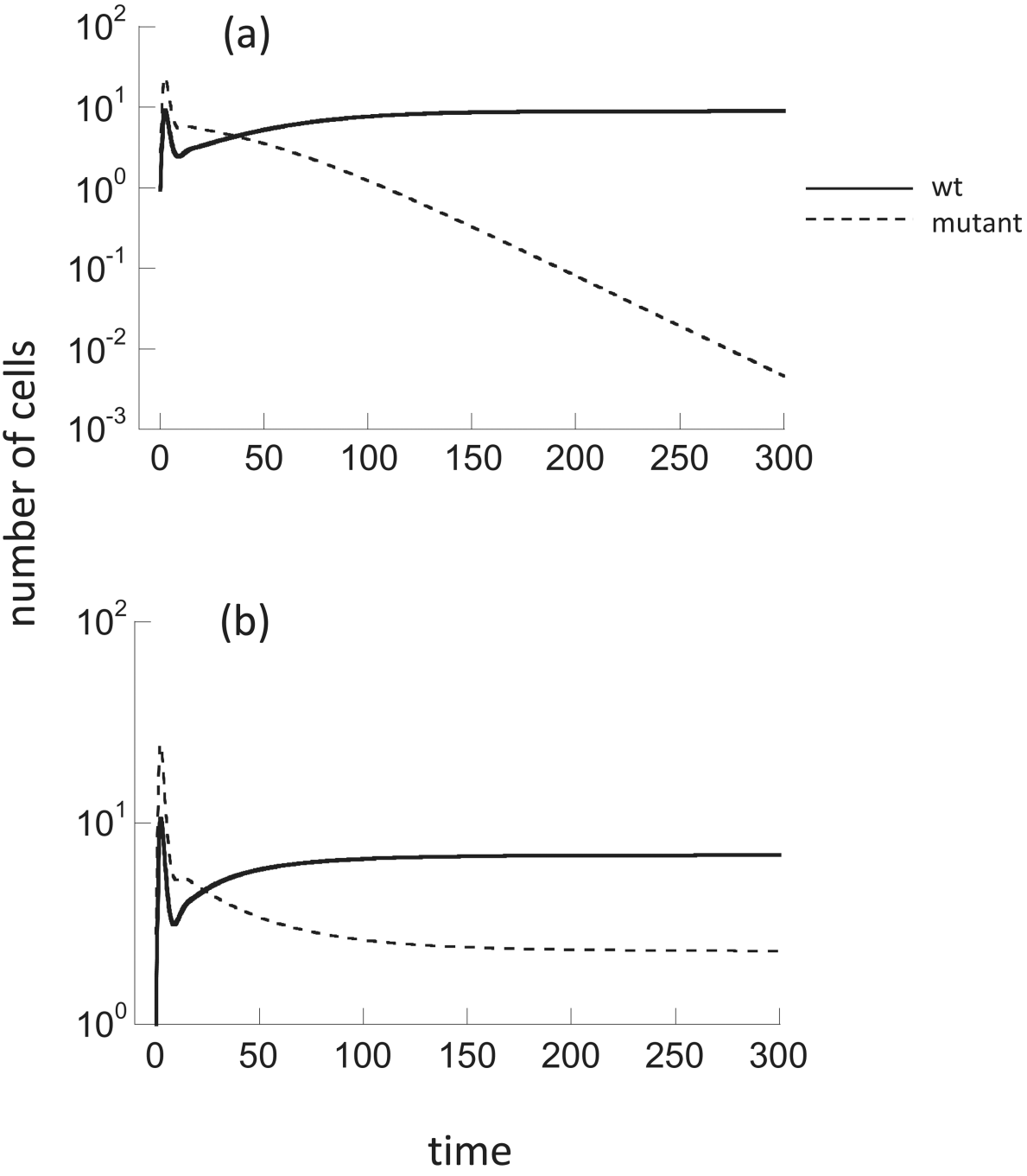

Figure 3.

Outcomes of the competition model (2). (a) Competitive exclusion. (b) Coexistence. Parameters were chosen as follows. λ=10; d=0.1; β=0.1; k_1=1; k_2=0.95; u=1; ε=0. For (a) c=1, for (b) c=0.7. Not that the only difference between the two strains was assumed to lie in the rate of virus production, *k*. Infection cascade length n=100.

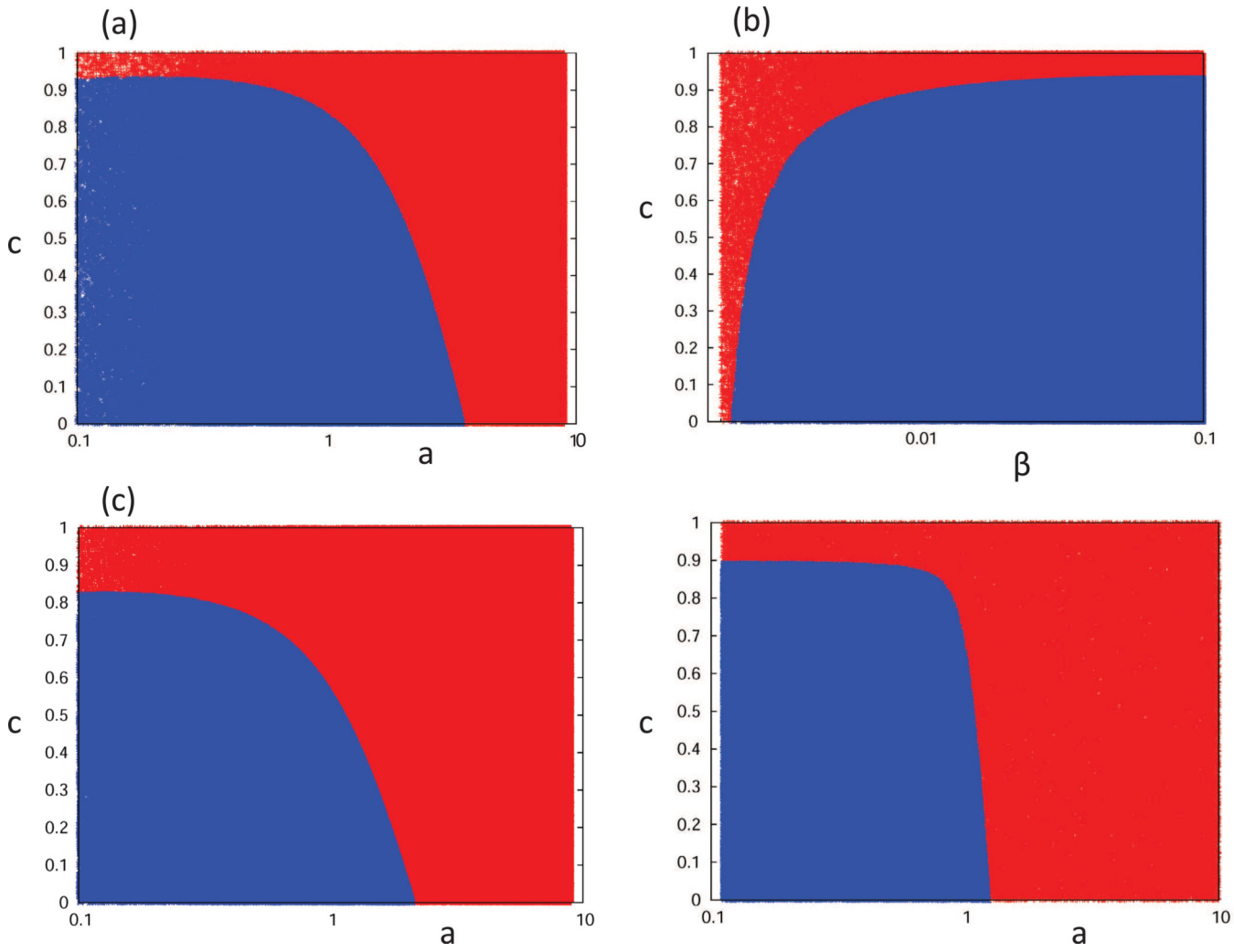

Figure 4.

Outcome of competition in model (2), depending on parameters that determine the rate of virus spread, and the parameter *c*, which describes the relative strength of intracellular competition among the two virus strains. Blue indicates coexistence, while red indicates exclusion of the inferior mutant by the wild-type. Results are based on numerical simulations. (a) Effect of the death rate of infected cells, assuming that the mutant has a 5% fitness cost compared to the wild-type virus. The higher the death rate of infected cells, the slower the spread of the virus, and the more difficult it is to observe coexistence. That is, for higher values of *a*, coexistence requires a lower value of *c*, i.e. more intracellular niche separation. If the value of *a* lies above a threshold, coexistence is impossible. (b) Effect of the rate of infection, assuming a 5% fitness cost. The lower the rate of infection, the more difficult it is to observe coexistence. (c) Same as (a), but with a 15% fitness cost, which reduces the coexistence regime. (d) Same as (a), but assuming increased viral output in multiply infected cells. Now, the coexistence regime is larger. Parameters were chosen as follows. λ=10; d=0.1; a=0.2; β=0.1; k_1=1; u=1. For (a,b) k_2=0.95; ε=0. For (c) k_2=0.85; ε=0. For (d) k_2=0.95; ε=50. Infection cascade length n=100. Larger infection cascade lengths (up to n=500) were also explored and did not change the results plotted here. These simulations

were computationally much more costly, were not run to include as many data points, and are hence not shown.

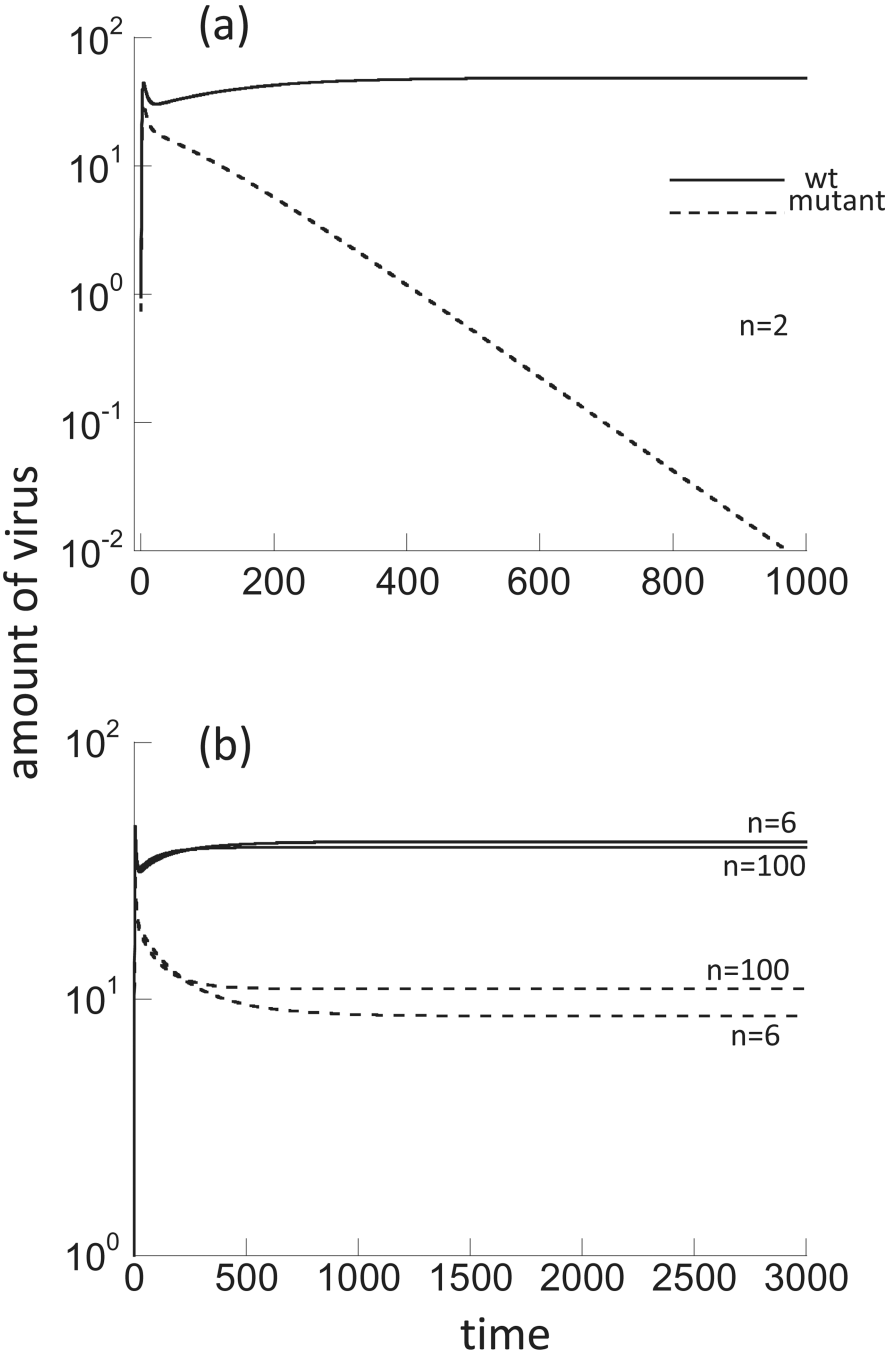

Figure 5.

Dependence of the competition outcome in model (2) on the length of the infection cascade, *n*. (a) For n=2, numerical simulations lead to competitive exclusion. (b) For higher values of *n*, coexistence is observed. However, the equilibrium population values to which the simulations converge can depend on the exact length of the infection cascade. Thus, when studying the competition dynamics with this model, it is important to make sure that parameter regions are considered where the length of the infection cascade does not influence outcome or equilibrium values in numerical simulations. Parameters were chosen

as follows. $\lambda=10$; $d=0.1$; $a=0.2$; $\beta=0.1$; $k_1=1$; $k_2=0.95$; $u=1$; $c=0.9$, $\varepsilon=0$. Cascade lengths are indicated in the figure.

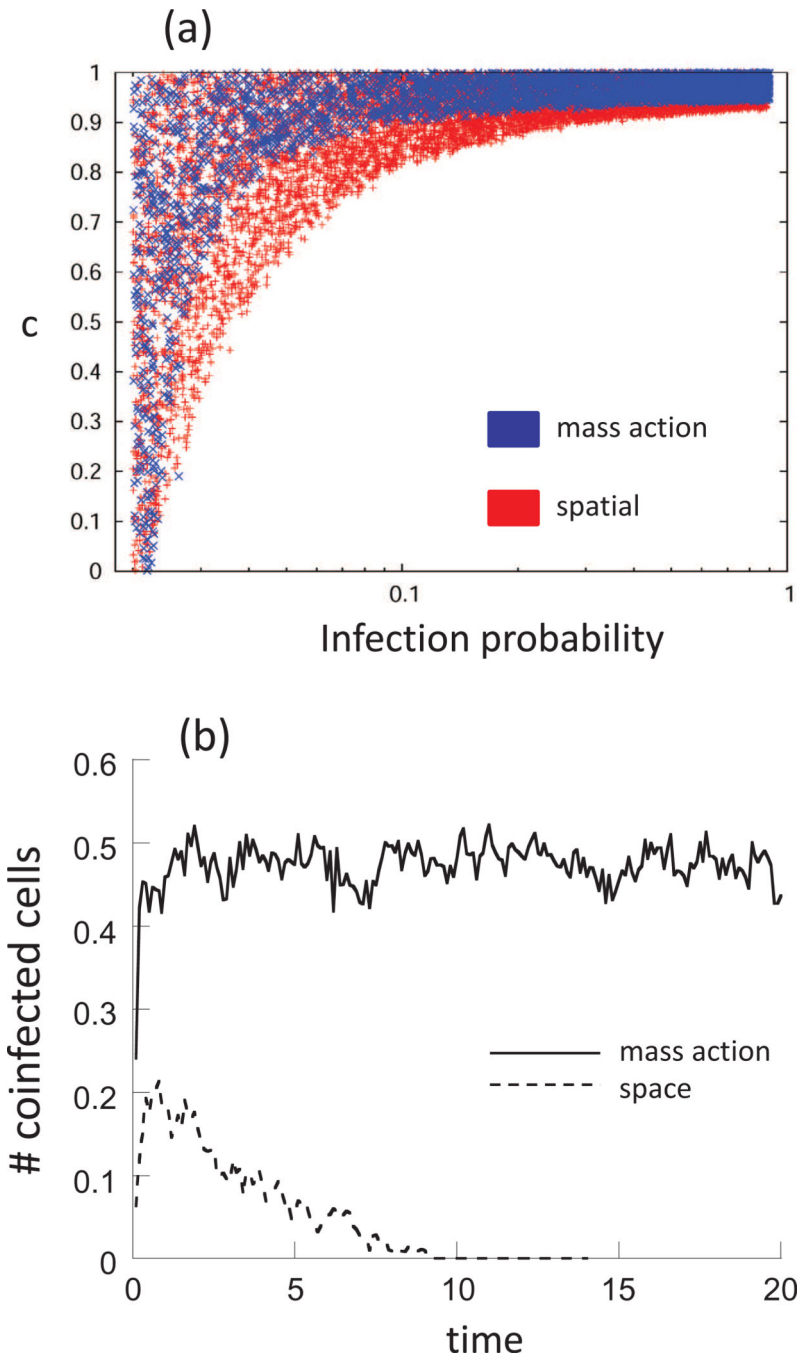

Figure 6.

(a) Competition in spatial (nearest neighbor) versus non-spatial (mass-action) settings, using the agent-based model described in the text. Only the extinction parameter region is plotted, both for the spatial (red) and mass-action (blue) settings, depending on the infection probability *B* and the intracellular competition parameter *c*. Because in stochastic simulations, population extinction will occur if the simulation runs for a sufficiently long period of time, the outcome of competition was determined as follows. Initial conditions were used in which spontaneous extinction of either virus in isolation was very unlikely.

One hundred infected cells of each type were seeded randomly across the grid. If the inferior strain went extinct before a time threshold, the outcome was recorded as competitive exclusion. Otherwise, the outcome was recorded as coexistence. The time threshold was chosen such that the outcome did not change if the duration of the simulation was increased further. As mentioned in the text, the spatial and the non-spatial simulations have different infection rate thresholds for establishment of infection. To directly compare the size of the extinction regimes in the two settings, we subtracted the difference in the threshold values from the infection probability parameter in the spatial simulations. Parameters were chosen as follows. L=0.8; D=0.01; A=0.02; ε=0. The grids size was 50×50. (b) Reason for the larger extinction region in the spatial simulation. In the spatial setting, fewer cells are generated that contain both virus strains than in the mass-action setting, accounting for the larger extinction regime. Parameters were chosen as follows. L=0.8; D=0.01; A=0.02; B=0.0623; c=0.73; ε=0. The grids size was 50×50.